

HYPERBOLIC PDES ACROSS GASDYNAMICS, PLASTICITY, AND GRANULAR PLASTICITY

PETER HOFFMAN

(Communicated by M. Neda)

Dedicated to Professor William J. Layton on the occasion of his 60th birthday

Abstract. This expository paper is presented in celebration of Professor Layton's 60th birthday. In mathematics genealogy, he is the gg-grandson of Göttingen's Ludwig Prandtl (1875-1953), who contributed enormously to both fluid and solid mechanics. The Prandtl-Meyer fan is a simple tool to visualize solutions of hyperbolic PDEs in the context of gasdynamics. In later years, Prandtl adapted the fan to visualize solutions of hyperbolic PDEs in the context of plasticity in metals. By 1960, the fan had been used by Sokolovskii in the context of granular plasticity. Because the last introduces logarithms into plasticity's equivalent of the Riemann invariant, granular materials exhibit unexpected behaviors that are being ignored by the construction community with costly consequences. Interestingly, one of the consequences for soil is analogous to the Rankine-Hugoniot relation in gasdynamics.

Key words. Prandtl fan, gasdynamics, plasticity, granular plasticity, Euclidean

1. Introduction

Hyperbolic partial differential equations (PDEs) provide the common framework that facilitated work by Prandtl, his students, and his colleagues as they moved among the disciplines of gasdynamics, plasticity, and granular plasticity:

- Gasdynamics involves compressibility, and it usually involves high speed flow where shocks and other compressibility effects are evident.
- Plasticity is contrasted with elasticity; that is, an elastic object regains its shape after a load is removed, but in plasticity, it does not. Plasticity applies to metal forming.
- Granular plasticity describes gritty materials that exhibit internal friction, such as salt, soil, concrete, and exotic metals[5]. Examples of its application are provided later.

This paper explores analogies among these disciplines and their PDEs. Gasdynamicists understand the difference between the Euler equation and the Navier-Stokes equation. The former is inviscid, and the latter includes viscous effects. Similarly, plasticity is inviscid, and granular plasticity includes viscous effects; that is,

Euler Eq : Navier-Stokes Eq :: plasticity : granular plasticity

This analogy ignores boundary friction in plasticity, which must be countered by lubricants during metal forming. In contrast, the friction of granular plasticity is internal friction everywhere within the material.

The Euler and Navier-Stokes equations are evolution equations, and they are solved by marching in time. Plasticity uses strain rate, not time, but strain became a point of dispute between plasticity and granular plasticity. This dispute, which

is associated with plasticity's Normality Rule, will be discussed. Therefore, time is avoided, and steady-state equations are used here. For steady-state inviscid PDEs, consider this analogy,

elliptic : hyperbolic :: subsonic : supersonic :: elastic : plastic

Graphically, these analogies are emphasized by the Prandtl-Meyer fan and its adaptation across the disciplines.

2. Gasdynamics

Before the supercomputer, numerical solution of conservation laws and evolution equations was usually impractical.

2.1. Since 1977: Evolution Equations. Computing caused a revolution in mathematics, but Seymour Cray, the person at the center of the revolution, knew nothing about the math of gasdynamics other than the importance of linear algebra... fast linear algebra.

Before building his Cray 1 in 1977, he had humiliated IBM by breaking the MFLOP barrier with the CDC 6600. This prompted IBM CEO Thomas J. Watson to write a famous, and angry, memo to his employees [9]:

Last week, Control Data... announced the 6600 system. I understand that in the laboratory developing the system there are only 34 people including the janitor... Contrasting this modest effort with our vast development activities, I fail to understand why we have lost our industry leadership position by letting someone else offer the world's most powerful computer.

With the advent of high-performance computing in 1977, long after World War II, time-dependent conservation laws became the focus. In gasdynamics, these conservation laws are called the Euler equations, and they express conservation of mass, momentum, and energy. As computer power further increased, researchers added chemistry or tackled the Navier-Stokes equations. The latter disturb conservation with viscosity, which gives the dissipative, but interesting, effects of boundary layers and turbulence.

2.1.1. Example: Space Shuttle Orbiter. The first orbital flight of the Space Shuttle occurred in 1981. The orbiter's behavior differed greatly from wind tunnel predictions [1]:

Flight experience with the shuttle has indicated a much higher pitching moment at hypersonic speeds than predicted; this has required the body flap deflection for trim to be more than twice that predicted.

Adding drama, Bertin and Cummings [3] emphasized that the required flap angle was...

...close to the limit of possible deflection.

The difference was explained because an early Cray computer, shared across America by phone lines, enabled the inclusion of high temperature air chemistry within a flow calculation by Maus and others [15]. This episode became a famous textbook example decisively showing that computations could provide an alternative to wind tunnels [1].

At the time, each and every bit of memory required a worker to thread copper wires through a tiny iron donut. With memory and speed limitations, early computations made compromises with (1) complex physics, (2) complex geometry, and (3) time evolution. Computers of the early 1980's required users to choose one from these three desired capabilities, but a focused industry made rapid progress over the next two decades.

2.2. Before 1977: Steady-state Equations. Before computers, Prandtl and his students were limited to hand calculations. Being hyperbolic PDEs, the Euler equations are amenable to hand solution by the method of characteristics; that is, certain quantities (Riemann invariants) are constant in certain directions (characteristics). But, time evolution is tedious, and a computer is a convenient, perhaps necessary, tool for capturing a shock.

It is easily forgotten that, from the groundwork of the Euler equations, one can derive steady-state first-order PDEs that, too, are hyperbolic when the flow is supersonic. Rather than evolving in time, solutions can be marched spatially. For Prandtl, hand calculations with the spatially-marched method of characteristics provided solutions for nozzles, ramps, and other simple geometries [14].

The Prandtl-Meyer fan describes the characteristic net of the expansion zone. As Prandtl's student at Göttingen, Meyer graduated in 1908 with a dissertation entitled *ber zweidimensionale Bewegungsvorgänge in einem Gas, das mit Überschallgeschwindigkeit strömt* [About two-dimensional movement in a gas flowing at supersonic speed] [16].

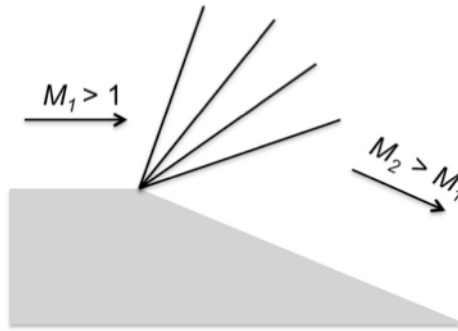


FIGURE 1. Notional Prandtl-Meyer fan for expansion in supersonic flow.

Designing the large supersonic wind tunnels of the 1950s, the US Air Force had enlisted German scientists to supervise hand calculations. They used the steady-state method of characteristics, recorded with enormous sheets of paper on the floor of an aircraft hangar [7].

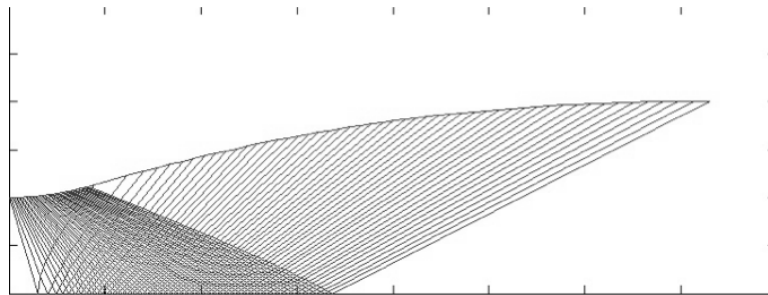


FIGURE 2. Smooth expansion creates a test section (rhombus) of uniform Mach number.

Providing a range of Mach numbers, the Air Force tunnels were designed with flexible nozzles controlled by an early computer, the ERA 1102. They were the first

use of industrial control, now called robotics [19]. Furthermore, Seymour Cray had been a pioneering computer engineer at Engineering Research Associates (ERA). Since Cray's death twenty years ago, the world has learned that ERA had been involved, like Alan Turing and Bletchley Park, in World War II codebreaking. The American codebreakers included Harvard's logician Quine and topologist Gleason. Although dedicated to the Manhattan Project, Princeton's von Neumann advised on computing, and the von Neumann architecture originated in WWII.

3. Plasticity

Prandtl inaugurated the modern study of plasticity when he applied the fan to metal-forming [20].

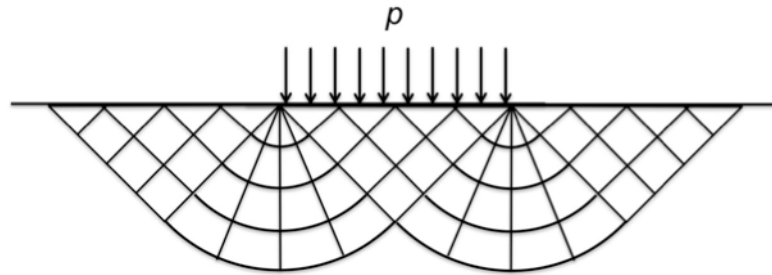


FIGURE 3. With sufficient pressure p , a die indents and displaces metal along characteristics. This characteristic net connects three 45° triangles with two Prandtl fans.

Felix Klein (1849-1925) and Otto Mohr (1835-1918) were among Prandtl's mathematical grandfathers. Using statics, Mohr studied the nature of stress in a solid. Stress is represented by a symmetric matrix, which has real eigenvalues. The largest and smallest eigenvalues are called the major and minor principal stresses, which act in principal directions or eigenvectors that are orthogonal. Plasticity in metals occurs when shear stress is a maximum; that is, it occurs in directions that are 45° from principal directions. In 2D, the difference between major and minor principal stresses is identified with deviatoric stress. Engineers are taught that "Mohr's circle" expresses invariance of the deviatoric stress. Klein promoted these geometric characterizations, and he even taught mechanics himself as he constructed the program at Göttingen. Klein recruited the mathematician Hilbert, physicist Sommerfeld, and engineer Prandtl. Göttingen's reputation in mechanics remained unrivaled until World War II.

The plasticity equations describe incipient plasticity, which is the moment after departure from elasticity but before equilibrium has been disturbed. The equations combine a geometric description of plasticity involving Mohr's circle with an assertion of equilibrium, namely Cauchy's equation for spatial variation of the stress matrix, Σ , in the absence of gravity and body forces,

$$(1) \quad \operatorname{div} \Sigma = 0$$

In two dimensions, this gives two scalar equations, that is, a system of two first order PDEs that reduces to ordinary differential equations (ODEs) along characteristics. The characteristics are lines of plastic slip, and the ODEs yield the analog of Riemann invariants.

Using the plasticity invariants, one finds that the angle α of Prandtl's fan determines the capacity $p_1 = (1 + \alpha)F_y$ of a metal shape [10].

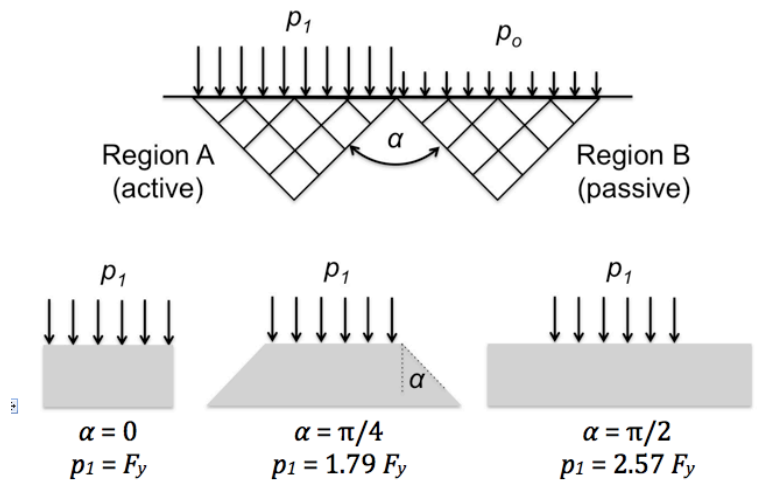


FIGURE 4. Angle α of Prandtl's fan determines the capacity $p_1 = (1 + \alpha)F_y$ of a metal shape. Sloped side increases capacity. The active region pushes while the passive region is pushed.

Metals are called *von Mises* materials. Having received a doctorate from Vienna in 1908, Richard von Mises (1883-1953) designed aircraft for Austria during World War I and created an institute for applied mathematics at the University of Berlin.

In 1921, Prandtl and von Mises co-founded the *Gesellschaft für Angewandte Mathematik und Mechanik (GAMM)* [Society for Applied Mathematics and Mechanics] and the journal, *Zeitschrift für Angewandte Mathematik und Mechanik (ZAMM)*.

Von Mises wrote ZAMM's first article [27], *Zur Einführung: Über die Aufgaben und Ziele der angewandten Mathematik* [Introduction: On the Tasks and Objectives of Applied Mathematics]. And, Prandtl wrote the second, *Über die Eindringungsfestigkeit (Härte) plastischer Baustoffe und die Festigkeit von Schneiden* [On the Penetration Resistance (hardness) of Plastic Materials and the Strength of Cutting], which founded modern plasticity theory.

With Hitler's rise, von Mises fled and became professor of aerodynamics at Harvard.

4. Granular Plasticity

Granular materials are identified as *Mohr-Coulomb* materials, despite the fact that Coulomb (1736-1806) had investigated both plasticity (metal) and granular plasticity (soil).

Granular plasticity introduces friction. In order to slide a block of weight W across a surface, a force F is required. The coefficient of friction is $\mu = F/W$. Force F is tangential, and force W is normal to the surface. Suppose the surface

is inclined. The block's weight W can be resolved into a components normal and tangential to the surface. As the angle of inclination is increased, there will be an angle ϕ when the block slides. The tangential force is $W \sin \phi$, and the normal force is $W \cos \phi$. The coefficient of friction is the ratio of tangential and normal forces; thus,

$$(2) \quad \mu = \frac{W \sin \phi}{W \cos \phi} = \tan \phi$$

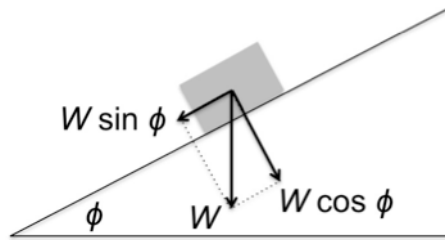


FIGURE 5. Friction angle, ϕ .

Angle ϕ is called the friction angle. For aggregates, ϕ represents the angle of internal friction among individual particles. Laboratory tests, called triaxial tests, are used to determine friction angles. However, the angle determined in the lab is approximated by the angle of repose, the angle with the horizon formed by the slope of a heap of aggregate.

Using stresses, the friction coefficient is

$$(3) \quad \frac{\tau A}{\sigma A} = \tan \phi$$

where τ = shear stress and σ = normal stress on a plane where sliding or soil failure occurs, i.e., at plasticity. When cohesive or von Mises strength, k , is included, one has Coulomb's equation,

$$(4) \quad \tau = k + \sigma \tan \phi$$

When Coulomb's equation is included in the plasticity equations, the resulting PDE system is general but messy [10]. Here, ϕ = the friction angle, θ = orientation of principal directions or stress eigenvectors, k = cohesion or von Mises yield stress, and $p = \text{trace}(\Sigma)/2$ = mean stress in two dimensions.

$$(5) \quad \begin{aligned} & (1 + \sin \phi \cos 2\theta) \frac{\partial p}{\partial x} + \sin \phi \sin 2\theta \frac{\partial p}{\partial y} \\ & = 2(k \cos \phi + p \sin \phi) \left(\sin 2\theta \frac{\partial \theta}{\partial x} - \cos 2\theta \frac{\partial \theta}{\partial y} \right) \\ & \sin \phi \sin 2\theta \frac{\partial p}{\partial x} + (1 - \sin \phi \cos 2\theta) \frac{\partial p}{\partial y} \\ & = -2(k \cos \phi + p \sin \phi) \left(\cos 2\theta \frac{\partial \theta}{\partial x} + \sin 2\theta \frac{\partial \theta}{\partial y} \right) \end{aligned}$$

Equation (5) is formidable, but some easy observations are possible:

- The equation results from inclusion of simple information into $\text{div } \Sigma = 0$.
- The equation simplifies greatly for the ordinary plasticity ($\phi = 0$) case.
- θ is always preceded by 2, but ϕ is not.

The last observation is *central* to this paper and to the Normality Rule dispute, which will be discussed.

Four decades elapsed between Prandtl's solution for ordinary plasticity and the solution by Sokolovskii (1912-1978) for general plasticity [22]. The transfer of plasticity knowledge to Russia, from Prandtl's circle of colleagues in Germany, is attributed to Heinrich Hencky (1885-1951), who had fled from Hitler.

For granular or Mohr-Coulomb plasticity, the characteristics are no longer inclined 45° from principal directions or stress eigenvectors.

	von Mises	Mohr-Coulomb
characteristics	$\pm 45^\circ$	$\pm 45^\circ \pm \phi/2$
invariants	$p \pm 2k\theta$	$\ln(k + p \tan \theta) \pm 2\theta \tan \phi$

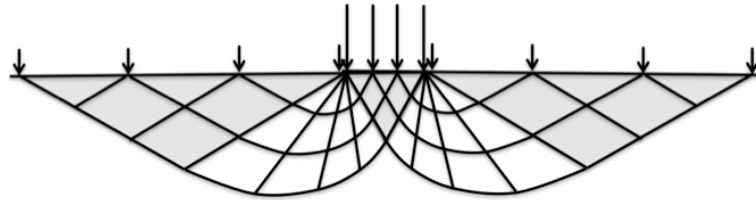


FIGURE 6. A net of characteristics for a granular material. Prandtl's fan now has a log spiral, not a circular arc. Construction of a building heaves adjacent buildings. A sinking building tilts, one way or the other, in order to follow characteristics.

Today, Sokolovskii's granular plasticity solution is used to determine soil bearing capacity for structures that range from houses to North Sea oil platforms [6,25].

5. Angles of Characteristics and Concepts of Pressure

The 2D method of characteristics tracks an invariant along a characteristic. When two characteristics intersect, the two invariants provide two equations that determine two quantities. In gasdynamics, the method of characteristics involves bookkeeping of quantities such as angle θ and Mach Number M . In both plasticity and granular plasticity, the bookkeeping involves an angle θ and a pressure p as the solution marches from point to point.

Using the isentropic relations of gasdynamics, Mach number could be replaced by pressure. Then, the method in all three disciplines could be viewed as marching (θ, p) forward.

However, the definitions of θ and p differ between gasdynamics and plasticity. In plasticity, p is mean pressure associated with the trace of the stress matrix. In gasdynamics, p is mean pressure by default because p is the same in every direction.

In gasdynamics, θ is an angle associated with flow direction and determined, for example, by the geometry of a wind tunnel. In plasticity, θ is an angle associated with direction of the major principal stress.

Angles are important: they are subtly disturbed by friction and, according to Prandtl-Glauert theory in gasdynamics [14], by viscosity. *Concepts of pressure are important:* they reflect transitions among elasticity, plasticity, and fluidity.

6. Plasticity Overview

Reflecting fifty years of history, this section examines unification, separation, and re-unification of ordinary and granular plasticity.

6.1. Unification. The granular plasticity solution for Mohr-Coulomb materials is general, and when $\phi = 0$, it simplifies to Prandtl's plasticity solution for von Mises materials, e.g., common metals.

While Hencky took plasticity theory to Russia, William Prager (1903-1980) brought it to the United States. At the age of 26, Prager had been Director of the Institute of Applied Mathematics at Göttingen. He was removed when the Nazis came to power. Most professors at Göttingen were eventually removed because they were Jewish or had Jewish connections, and they were replaced by Nazi party functionaries. The elderly Prandtl was highly regarded by the party, but between 1938 and 1941, he was driven by frustration to protest to Göring and Himmler regarding Nazi disrespect for Göttingen. Prandtl's daughter provides evidence of these events in her biography [26].

At Brown University, Prager and Daniel Drucker (1918-2001) created the Drucker-Prager plasticity model, a unified view that included both von Mises and Mohr-Coulomb materials [10]. This paper has already been using *granular plasticity* and *general plasticity* interchangeably.

Recently, exotic metals of exceptional strength have been created by doping common metals with nanoparticle granules [5]. Their capacity and behavior are described by the granular plasticity solution where $k =$ von Mises yield stress.

6.2. Separation. Unfortunately, over the last fifty years, Mohr-Coulomb plasticity diverged from von Mises plasticity. The reason for divergence is the Normality Rule, a consequence of the Drucker Stability Postulate. The rule says that plastic strain ϵ^p must be normal to the failure surface in stress space, which is the 2D space where Cartesian pairs (σ_1, σ_3) are the major and minor principal stresses. 3D stress space consists of Cartesian triples $(\sigma_1, \sigma_2, \sigma_3)$, but in 2D, convention drops σ_2 .

The Normality Rule is not directly applicable to granular materials. In recent decades, granular materials have been designated *non-standard* with *non-associated plastic potentials*. Logically, this would also appear to invalidate the Drucker Stability Postulate, from which the Normality Rule follows. Drucker Stability associates deformation with non-negative work.

6.3. Re-unification. Despite being designated non-standard, Mohr-Coulomb materials cannot escape the laws of physics, and in 2014, Sun [23] proved the Drucker Stability Postulate, making it a theorem. His proof uses differential forms and follows from the Poincaré lemma. In turn, the Poincaré lemma assumes a star-shaped or simply-connected domain; that is, it must idealize a material as a continuum without holes, which could collapse and absorb energy.

For granular or Mohr-Coulomb materials, the Normality Rule is not directly applicable because stress space is non-Euclidean and angles are skewed. Superficially, stress space $\sigma_1\sigma_3$ resembles Euclidean xy space; however, stress space geometry is distorted. Slopes of lines are m^2 when they should be m . *The PDE of equation (5) hints of this distortion because θ is always preceded by two;* that is, the physical angle (θ) differs from the mathematical angle (2θ).

In stress space, the yield surface of a granular material is shaped like an ice cream cone. For stress states inside the cone, the material is elastic. The surface itself corresponds to plastic behavior.

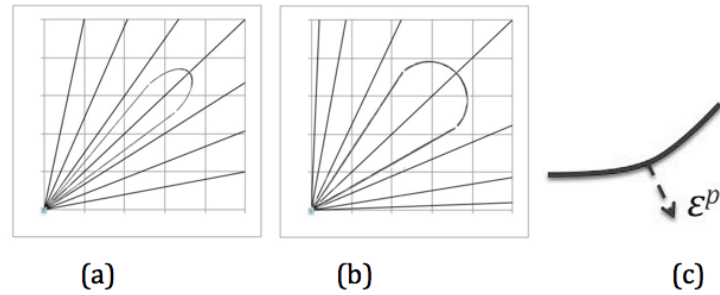


FIGURE 7. A yield surface, shaped here as an ice cream cone, is shown as a narrow cone in (a) Euclidean space and as a wide cone in (b) stress space. A line with slope m in Euclidean space has slope m^2 in stress space. Plastic strain ϵ^p is normal (c) to the yield surface in Euclidean space, not in stress space as traditionally expected.

Non-Euclidean distortion is associated with dilatancy; that is, before one rough surface can slide over another, they must be separated slightly. In current finite element software for granular plasticity, dilatancy is treated as a vaguely-defined correction factor. While it gives reasonable results, it does not give accurate results for the matrix algebra broken by non-Euclidean geometry [11].

Test data for dilatancy validate analysis based on non-Euclidean distortion [12]. They re-establish belief that Drucker and Prager were correct fifty years ago.

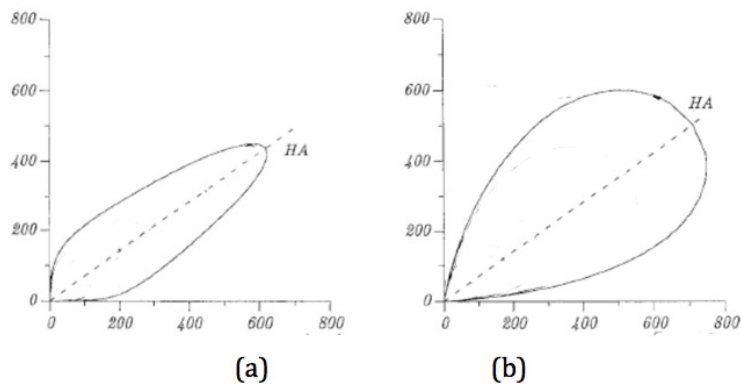


FIGURE 8. Test data in figures 8(a) and 8(b) show narrow and wide surfaces that validate the analytical relationship between figures 7(a) and (b). The wide surface in (b) is the yield surface. Transformed back to Euclidean space in (a), the narrow surface is called the *plastic potential*.

7. Application to Reinforced Soil

Reinforced soil in granular plasticity resembles, except for internal friction, the metal-forming of automobile fenders in ordinary plasticity. Both involve material sandwiched by stiffer material.

Engineered reinforced soil was invented in France fifty years ago by Schlosser and Vidal [21]. Sheets or strips of reinforcement are placed in the soil. In practice, it has supplanted traditional retaining walls, especially for high walls.

In recent years, reinforced soil has become ubiquitous. A casual observer may think, “Wow, that concrete is holding back that huge mass of soil.” The truth is quite the opposite: the soil is supporting a non-structural concrete facing.

This section examines three current successes and three failures with reinforced soil. Of course, many failures were originally hailed as successes.

7.1. Three Successes.

7.1.1. Denver Airport Commuter Rail. Denver has challenging soil. It had to be addressed by designers of the new commuter rail between the airport and downtown. The figure shows how reinforcement interrupts the Prandtl fan beneath the rail car. In this case, the reinforcement is fiberglass.

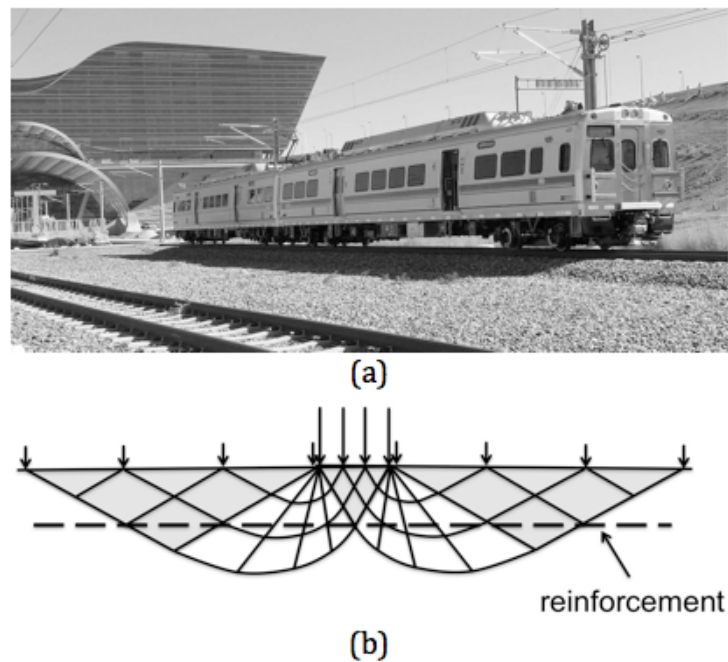


FIGURE 9. Soil beneath (a) new commuter rail to Denver’s airport is stabilized with (b) reinforcement that prevents plastic slip along characteristics.

7.1.2. Overpass near Denver Airport. Near Denver’s airport, a transcontinental highway crosses a transcontinental railroad. The bridge had reached its end of life, and the highway needed widening. Complicating the bridge replacement, an underground pipeline carries jet fuel to the airport. Piles were driven to support

the bridge's west end, but reinforced soil supports its east end. Reinforcement is a polypropylene geosynthetic.



FIGURE 10. New triple-span bridge on I-70 over the transcontinental railroad near Denver's airport. The east end (right) is supported by reinforced soil. Pipeline marker is in foreground.

7.1.3. Sea-Tac Airport's High Wall. Expansion of the airport for Seattle and Tacoma required a 150 foot high earth retention structure. Extremely high retaining walls are infeasible; instead, designers used reinforced soil. The soil is reinforced with galvanized steel strips, and concrete facing panels are attached. Sea-Tac is located in a zone of high seismic activity.

7.2. Three Failures and an Explanation.

7.2.1. Explanation. Prandtl's fan has been used as a common thread illustrating hyperbolic PDEs across gasdynamics, von Mises plasticity, and Mohr-Coulomb plasticity. There is no obvious association of the fan with failures, and one must return to characteristics.

Consider a layer of reinforced soil. As shown, θ is a function of shear stress between soil and reinforcement. Near mid-layer, shear stress is zero; therefore, $\theta = 0$. This follows because magnitude of shear at the top of the layer approximates that at the bottom and because *their signs are opposite*.

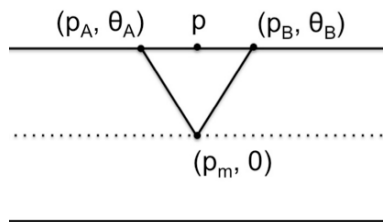


FIGURE 11. Characteristics connect mid-layer point p_m with two points near reinforcement.

Characteristics connect Points A and B with the point at mid-layer. By the invariants, if soil friction angle $\phi = 45^\circ$,

$$(6) \quad \begin{aligned} \ln p_m &= \ln p_A - 2\theta_A \\ \ln p_m &= \ln p_B + 2\theta_B \end{aligned}$$

Addition gives

$$(7) \quad \begin{aligned} 2 \ln p_m &= \ln p_A + \ln p_B - 2(\theta_A - \theta_B) \\ \ln p_m &= \ln(\sqrt{p_A p_B}) - \Delta\theta \end{aligned}$$

Approximating p with the geometric mean, $\sqrt{p_A p_B}$,

$$(8) \quad \begin{aligned} \ln p_m &= \ln p - \Delta\theta \\ \ln(p_m/p) &= -\Delta\theta \\ p_m/p &= e^{-\Delta\theta} \end{aligned}$$

The pressure's exponential behavior, derived here, is due to a difference in shear $\Delta\theta$ and is called *shear lag* W . It leads to instability; that is, it leads from elasticity to plasticity and, eventually, to fluid behavior where W or resistance to shear vanishes. It can be shown by a free body diagram that the difference in shear $\Delta\theta$ is proportional to S/D where S is reinforcement spacing and D is size of granules in the material.

Interestingly, shear lag was investigated by von Kármán in 1923 in the context of von Mises materials [24]. In the context of Mohr-Coulomb materials, it was validated by tests performed at the Federal Highway Administration (FHWA) lab in McLean, VA [11,18,28,29]. At large S/D , resistance to shear vanishes in accord with Mohr's circle, stress matrix eigenvalues coalesce, and fluid behavior emerges.

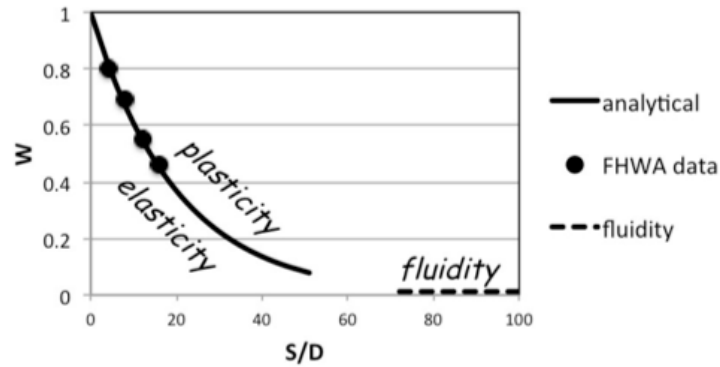


FIGURE 12. FHWA test data confirm S/D instability based on the exponential equation derived by the method of characteristics from plasticity theory. Fluid behavior emerges at bottom right; that is, resistance to shear vanishes.

At large S/D , validation of fluid behavior is supported by a previous figure, 8(a). The contour, determined experimentally at large S/D approaches the origin along the axes.

To gasdynamicists, Figure 12 resembles a diagram of transition to turbulence with Reynolds number $Re = UL/\nu$, where U is velocity and ν is kinematic viscosity. The dimensionless parameter S/D is analogous to Reynolds number. Interestingly, both gasdynamics and granular plasticity associate instability with an external length, L or S .

Although confronted with FHWA lab data, the construction lobby demands that the status quo be maintained because an updated standard would cause “confusion” [2]. Causation will be argued for years, but the following failures are associated with large S/D .

7.2.2. \$5M Failure: Collapsed Overpass. An overpass in British Columbia used steel welded wire fabric as reinforcement. Large S/D and excessive reinforcement stiffness are associated with premature elastic-plastic transition. Failure occurred before completion [17].

The 2011 failure is analogous to the Rankine-Hugoniot phenomenon in gasdynamics. Transition causes an abrupt change in pressure. In the elastic state, pressure behind the concrete facing is negligible. With transition to the plastic state, pressure rises significantly, and the concrete facing is destroyed.

7.2.3. \$50M Failure: Yeager Airport Landslide. Charleston’s Yeager Airport is the largest in West Virginia. A 250 foot high reinforced soil structure provided a runway extension and overrun area. It had a large S/D . Its 2015 failure destroyed the 50-home community below.



FIGURE 13. Five years after its construction, collapse of a large reinforced soil structure at Yeager Airport, WV, destroyed the community below.

7.2.4. \$500M Failure: Millennium Tower. In 2016, newspapers reported that San Francisco’s 58-story Millennium Tower is sinking. Designers took measures to avoid the failure mode associated with a Prandtl fan. However, 200 feet of sand lie between bedrock and the building’s reinforced concrete base. This resembles reinforced soil where the bedrock and reinforced concrete act as reinforcement. Again, S/D is large.

8. Concluding Remarks

This expository paper tracks the Prandtl fan across *steady-state* gasdynamics, plasticity, and granular plasticity. Hopefully, correct *evolution equations* can be developed across these disciplines. Current methods and software ignore essential physical information.

Prandtl, along with his colleagues and students at Göttingen, practiced an astonishing range of math and mechanics. His mathematical family lists 87 students and more than 3510 descendants. Prandtl's students include:

- Ackeret - coined *Mach number*. At the University of Zurich, his students include von Braun, who led German and American rocket programs, and Liepmann, who wrote *Elements of Gasdynamics* and followed von Kármán as Director of the aeronautical laboratory at Cal Tech.
- Busemann - proposed swept wing design for high-speed aircraft, which was adopted in the Messerschmitt 262 and the Boeing B-47. (Without swept wings, breaking the sound barrier was rough in the early X-1. This enhanced Chuck Yeager's reputation.)
- Schlichting - wrote *Boundary Layer Theory*, a classic.
- Timoshenko - wrote the definitive textbook for mechanics of materials in the 20th Century. Similar classics had been written by Navier and by Föppl, who was Prandtl's teacher and father-in-law. All three made elasticity solutions, obtained from elliptic PDEs, accessible to students entering engineering.
- von Kármán - brought aerodynamics to maturity. He was Director of the aeronautical laboratory at Cal Tech from 1930 to 1949. In 1945, he recruited German scientists for the USA in *Operation Paperclip*.

Professor Layton is the mathematical g-grandson of Hanfried Ludloff, who left pre-war Germany and followed Hilbert's student Courant to NYU. Ludloff specialized in rotating flows and published 14 papers in English between 1940 and 1970. Evidence indicates that Ludloff may have been an acquaintance of dissident theologian Dietrich Bonhoeffer who was executed by Hitler's SS [4].

The author is fortunate to have met Professor Layton and his mentors, Professors Gunzburger and Dougalis, as supercomputing dawned in 1978. They mastered the numerical analysis of evolution equations [8,13].

9. Postscript and Discussion

Conference attendees suggested that *non-Euclidean* may not be the correct adjective for the stress space of a granular material in plasticity theory. *Non-Euclidean* connotes an exotic space, but *not Euclidean* would simply mean that angles are skewed. The search for the correct mathematical adjective continues.

At the conference, A.J. Meir, Professor at Southern Methodist University, informed the author of work by David Schaeffer, Professor at Duke University. Communication has now begun with Professor Schaeffer, and he approves reposting a comment from his website:

Although I worked in granular flow for 15 years, I largely stopped... I came to believe that the lack of well-posed governing equations was the major obstacle to progress in the field, and I believe that finding appropriate constitutive relations is a task better suited for physicists than mathematicians, so I reluctantly moved on.

Acknowledging the "obstacle to progress," this paper suggests a way to return, possibly, to the unified plasticity of Drucker and Prager.

References

- [1] Anderson, J.D., *Hypersonics and High Temperature Gas Dynamics*, AIAA, 2005.
- [2] Anderson, P.L., Gladstone, R.A., and Sankey, J.E., "State of the Practice of MSE Wall Design for Highway Structures," *Geotechnical Engineering State of the Art and Practice: Keynote Lectures for GeoCongress 2012*, Oakland, CA, 2012.
- [3] Bertin, J.J., and Cummings, R.M., "Critical Hypersonic Thermodynamic Phenomena." *Annual Review of Fluid Mechanics* 2006.
- [4] Bonhoeffer, D., and Barnett, V., *Dietrich Bonhoeffer Works, Volume 17*. Fortress Press, Minneapolis, 2014.
- [5] Chen, L-Y., Xu, J-Q., Choi, H., Pozuelo, M., Ma, X., Bhowmick, S., Yang, J-M., Mathandhu, S., and Li, X-C., "Processing and properties of magnesium containing a dense uniform dispersion of nanoparticles." *Nature* 528, 2015.
- [6] Das, B.M., *Principles of Geotechnical Engineering*. PWS Publishing Co, 1994.
- [7] Goethert, B.H. *Transonic Wind Tunnel Testing*. AGARD/NATO, Dover edition, 2007.
- [8] Gunzburger, M.D., *Perspectives in Flow Control and Optimization*, SIAM, 2002.
- [9] Hill, M.D., Jouppi, N.P., and Sohi, G.S., *Readings in Computer Architecture*. Morgan Kaufmann, San Francisco, 1999.
- [10] Hoffman, P.F., *Plasticity and the Mechanics of Reinforced Soil*. ISBN 1518873391, *Preservation Engineering*, 2015.
- [11] Hoffman, P.F., "Contributions of Janbu and Lade as applied to Reinforced Soil." *Proceedings of the 17th Nordic Geotechnical Meeting*, Reykjavik, 2016.
- [12] Lade, P.V., and Kim, M.K., "Single Hardening Constitutive Model for Frictional Materials III: Comparisons with Experimental Data." *Computers and Geotechnics* 6, 1988.
- [13] Layton, W.J., and Rebholz, L., *Approximate Deconvolution Methods of Turbulence*, Springer, 2012.
- [14] Liepmann, H.W., and Roshko, A., *Elements of Gasdynamics*. Wiley, New York, 1957.
- [15] Maus, J.R., Griffith, B.J., Szema, K.Y., and Best, J.T., "Hypersonic Mach Number and Real Gas Effects on Space Shuttle Orbiter Aerodynamics," *J. Spacecraft and Rockets*, 21:2, 1984.
- [16] Meyer, T., *Über zweidimensionale Bewegungsvorgänge in einem Gas, das mit Überschallgeschwindigkeit Strömt*, PhD. dissertation, Göttingen University, 1908.
- [17] Ministry of Transportation, "Westside Road Underpass Number 7558 Forensic Investigation of Failure of MSE Wall Facing." *British Columbia Ministry of Transportation and Infrastructure*, 2012.
- [18] Nicks, J.E., Adams, M.T., and Ooi, P.S.K., *Geosynthetic Reinforced Soil Performance Testing: Axial Load Deformation Relationships*. Report No. FHWA-HRT-13-066, Federal Highway Administration, McLean, VA, 2013.
- [19] Norris, W.C., *Interview with William Charles Norris*. Charles Babbage Institute, University of Minnesota, Minneapolis, 1986.
- [20] Prandtl, L., "Über die Eindringungsfestigkeit plastischer Baustoffe und die Festigkeit von Schneiden." *Zeitschrift für Angewandte Mathematik und Mechanik* 1, 1921.
- [21] Schlosser, F., and Vidal, H., "La Terre Armée." *Bulletin de Liaison des Laboratoires des Ponts et Chaussées*, No 41, 1969.
- [22] Sokolovskii, V.V., *Statics of Granular Media*. Pergamon, 1965.
- [23] Sun, B., "Rational Interpretation of the Postulates in Plasticity." *Results in Physics*, 4, 10-11, 2014.
- [24] Timoshenko, S.P., and Goodier, J.N., *Theory of Elasticity*, McGraw-Hill, New York, 1970.
- [25] Vanberg, M., Tefera, T., and Jahr, A., "Effect of pile sleeve opening and length below seabed on the bearing capacity of offshore jacket mudmats." *Proceedings of the 17th Nordic Geotechnical Meeting*, Reykjavik, 2016.
- [26] Vogel-Prandtl, J., *Ludwig Prandtl*. Universitätsverlag Göttingen, 2014.
- [27] Von Mises, R., "Zur Einführung: Über die Aufgaben und Ziele der angewandten Mathematik." *Zeitschrift für Angewandte Mathematik und Mechanik* 1, 1921.
- [28] Wu, J.T.H., and Payeur, J-B., "Connection Stability Analysis of Segmental Geosynthetic Reinforced Soil (GRS) Walls. *Transportation Infrastructure Geotechnology*, 2(1), 2014.
- [29] Wu, J.T.H. and Pham, T.Q., "Load Carrying Capacity and Required Reinforcement Strength of Closely Spaced Soil-Geosynthetic Composites," *J. Geotech. Geoenviron. Eng. ASCE* 139(9), 14681476, 2013.